PERFORMANCE DURING WHOLE BODY REACHING MOVEMENTS IS IMPAIRED IN HYPERGRAVITY WHILE PRESERVED IN MICROGRAVITY

L. Chomienne[1], P. Sainton[1], F. Sarlegna[1] and L. Bringoux[1]

[1]Aix Marseille Univ, CNRS, ISM, Marseille, France

Abstract

While recent findings demonstrated the importance of initial state estimates about gravity for optimized motor control, it remains unclear whether novel initial states are rapidly implemented movement planning (and control) in the same way when gravity is removed or increased. Here, we investigated the effect of microgravity and hypergravity exposure on whole-body reaching movements performed by standing subjects during parabolic flights. Reaching movements were analyzed regarding spatial accuracy (finger endpoint deviation), arm kinematics (arm angular displacement), whole-body kinematics (body bending) and EMG activity (muscular activation and synergies) of eight muscles. Results showed that kinematics and muscular activity are adjusted in microgravity allowing accurate whole-body reaching, thus confirming the perfectly scaled sensorimotor reorganization reported in previous recent studies. Contrasting with these observations, participants hardly reached the targets in 1.8g (systematic undershot). Strikingly, whole-body kinematics remained unchanged in hypergravity compared to 1g observations. Finally, while the analysis of synergies highlighted a comparable muscular organization in all gravitational contexts, our main findings revealed local muscular adjustments leading to accurate motor responses in microgravity, but not in hypergravity.

Introduction

Altered gravity causes a fundamental change of body dynamics to be integrated by the Central Nervous System (CNS) to maintain motor performance. This integration refers to the capacity of the CNS to modify the internal representation of the body according to environmental constraints. This process led to an adapted state which must be efficient in the new environment. Thereby, understanding how the CNS is able or not to produce and regulate efficient motor commands in microgravity and hypergravity remains a key issue in the field of human motor control.

As a major characteristic of our usual surrounding force field, Earth's gravity is optimally integrated by the CNS (Gaveau et al. 2021), the absence of gravitational field involves a substantial change in motor planning. Recent data collected during microgravity episodes of parabolic flights suggested that body unloading is taken into account in the planning of whole-body reaching movements before movement onset (Bringoux et al. 2020; Macaluso et al. 2017). Precisely, the consequences of the novel gravitational context on body dynamics are integrated by the CNS as an adapted state allowing adjusted motor actions (Bringoux et al. 2020; Gaveau et al. 2016; Macaluso et al. 2017; Rousseau et al. 2016). As such, from the very first exposure to microgravity during parabolic flights, endpoint performance of reaching movements was preserved even if kinematic adjustments were necessary to attain the target (Macaluso et al. 2017).

Although recently, unaltered motor performance has been generally reported in microgravity (White et al. 2020, for review), some studies revealed conflicting findings regarding motor responses in hypergravity. While few studies showed unaltered motor performance (e.g., movement accuracy; Crevecoeur et al. 2009a; Mierau et al. 2007), some others reported longer or partial sensorimotor reorganization on arm pointing (Bock et al. 1992; Gaveau et al. 2011) and grasping (Crevecoeur et al. 2014). For instance, Crevecoeur et al.

(2009a) highlighted perfectly scaled (within 3 trials) upward or downward arm movements in hypergravity (i.e., 1.8g) while Bock et al. (1992) highlighted a systematic overshot even after 20 parabolas of parabolic flight. The alteration of motor performance might be the consequence of the task and underlying mechanisms that could impact motor performance (Crevecoeur et al. 2009a).

Another issue raised in this study refers to the CNS ability to deal with unexpected and sudden perturbations in altered gravity. On Earth, the flexibility of sensorimotor control mechanisms is well known (Gomi 2008; Sarlegna and Mutha 2015, for reviews), as for instance motor commands can be rapidly adjusted during movement execution in response to a small mechanical (Cluff and Scott 2013; Crevecoeur and Scott 2013; Kimura and Gomi 2009) or visual (Chomienne et al. 2021; Hayashi et al. 2016; Saijo and Gomi 2010; Telgen et al. 2014) perturbation. In microgravity, Bringoux et al. (2020) reported that an unpredictable target jump triggered at arm movement onset did not affect final endpoint accuracy during a whole-body reaching task,. This finding highlighted the efficiency of visual feedback control in microgravity. It has been found however that adding a mass on the moving arm could impact endpoint accuracy in both microgravity and hypergravity (Bock et al. 1992). In microgravity, the CNS must adapt to body unloading, namely by an optimal integration of the absence of gravity for movement control (Gaveau et al. 2021). Nevertheless, whether changes in motor planning in response to novel gravitational contexts may lead to appropriate online regulations in response to unexpected mechanical perturbations remains an open question.

Here, we investigated the effect of microgravity and hypergravity on whole-body reaching movements. We asked standing subjects to reach with their dominant arm toward visual targets during parabolic flights. We recorded and analyzed joint kinematics to determine the multi-joint coordination patterns used in normo-, micro- and hypergravity. We also recorded and analyzed with surface electrodes the activity of 8 axial and distal muscles to characterize

the activation level and synergies in all 3 different gravitational contexts. We found that participants precisely reached the targets in microgravity by adjusting muscle activations and kinematics. In contrast, systematic undershots were observed in hypergravity, as a result of unchanged motor organization with respect to normogravity. Also, whatever the gravitational context, motor performance was maintained when an unpredictable mechanical perturbation was applied, suggesting that feedback control processes are efficient in microgravity as well as hypergravity.

MATERIALS AND METHODS

Participants

Nine right-handed volunteers (mean age = 30.8 ± 8.5 years, 4 women) participated in the study. They had no prior experience of parabolic flight and were naïve to the purpose of the study. None of the participants reported any neuromuscular or sensory impairments, as confirmed by a prior medical examination and all had normal or corrected-to-normal vision. Participants gave their signed informed consent prior the study in accordance with the Helsinki Convention. Before the parabolic flight, participants were given comfort medication (scopolamine) to avoid motion sickness. This medication has been shown to not alter sensorimotor control (e.g., reflex circuitry and muscular activation and coordination; Ritzmann et al. 2016). The study was authorized by the French National Agency for Biomedical Security (ANSM) and approved by the National Ethic Committee (CPP # 2015-A01231-48).

Apparatus

Participants stood upright, their feet were fastened to the cabin floor with foot-straps. A push-button located alongside their right body at arm length distance from the shoulder was used to standardize the starting fingertip position. In front of the participants, two LEDs-defined circular targets (diameter: 4 cm; Figure 1) were located relative to participant's anthropometry. A close target (Tclose) was set at shoulder's height at a distance corresponding to the arm length

and a far target (Tfar) was positioned 25 cm away and 20 cm below Tclose. Tclose and Tfar positions were arranged to investigate the arm and associated whole-body control (i.e., trunk displacement) during reaching, respectively. Participants wore a metal surface bracelet at the wrist positioned against an electromagnet located above the push-button (Figure 1) before movement onset. This device could generate a mechanical brake (pullout force: 60 N) at reaching initiation when the electromagnet was activated. The target lighting and electromagnet activation were recorded at 100 Hz and controlled by a homemade software (Docometre©) interacting with a real-time acquisition and control system (ADwin-Gold©, Jäger, Lorsch, Germany).

The 3D markers position (infra-red active markers) of head, shoulder, hip, knee, ankle, and index fingertip were recorded at 100 Hz with an optical motion capture system (Codamotion CXS and ActiveHub; Charnwood Dynamics, Leicestershire, UK) which allowed the tracking of both arm and whole-body displacement.

Surface electromyography (EMG) was recorded at 2000 Hz from 4 agonist muscles (Tibial Anterior, TA; Rectus Abdominis, RA; Deltoid Anterior, DA; lateral head of Biceps Brachii, BB) and 4 antagonist muscles (Soleus, SL; Erector Spinae, ES; Deltoid Posterior, DP; short head of Triceps Brachii, TB) involved in the whole-body reaching movements. Participants' skin was cleaned with alcohol and rubbed with an abrasive paper before affixing the surface electrodes (Ag-AgCl; diameter 1 cm, spacing 2 cm) along a line parallel to their fiber orientation to increase the signal-to-noise ratio (Brindle et al. 2006; Mills 2005).

Procedure

The study was carried out during the #142 parabolic flight campaign of the French national space research center (CNES) including 3 days of flight. The micro and hypergravity contexts were produced by a series of parabolic maneuver in a A-310 ZERO-G aircraft chartered by CNES and Novespace. The parabolic maneuver involved successive changes of

gravitational context that could be decomposed in three phases: 24 s of hypergravity (1.8g), 22 s of microgravity (0g) and 22 s of hypergravity (1.8g). The normogravity context (1g) was present during 1 min between each parabola. Each participant performed 15 trials (5 trials in 0g, 5 trials in 1.8g and 5 trials in 1g successively) for each of the 10 parabolas. The total of 150 trials was composed of 75 trials towards Tclose and 75 trials towards Tfar. In 20% of trials, the electromagnet generated a mechanical brake applied to the wrist at movement onset. Participants were informed of the possible occurrence of these perturbated trials but had no information regarding their sequencing. Targets and Perturbation (i.e., mechanical brake) conditions were presented in a pseudorandom order and counterbalanced between the participants.

The task consisted in reaching toward the target with the arm outstretched as fast and as accurately as possible when the target was switched on. Participants had to keep the final finger position until target extinction (3 s after movement onset) before returning to the starting position (i.e., upright standing, with the right index finger pressing the start push-button). Five trials in normogravity were performed by each participant during a 1-g steady state flight rest in the middle of the 10 parabolas and the experimental session lasted about 20 min.

Data processing

Data were analyzed using Matlab (Mathworks, Natick, MA). Raw positional data of kinematic markers were low-pass filtered with a dual-pass Butterworth (cut-off frequency: 10Hz; order: 3). Movement duration (MD) was identified as the time between movement onset and offset, identified when tangential velocity of index finger exceeded and fell below 2% of peak velocity (PV), respectively. The spatial accuracy of reaching movement was analyzed by computing the signed deviation along the longitudinal axis (z-axis) of the right index fingertip at movement offset. Positive and negative longitudinal endpoint error corresponded to overshot or undershot, respectively.

To analyze the arm kinematics during reaching movement, the arm angular elevation (i.e., angle evolution of the extended arm around the shoulder in the sagittal plane with respect to its initial orientation) was computed across time (Bringoux et al. 2020; Macaluso et al. 2016, 2017). From these values, the angular peak velocity (PVang) and its relative time of occurrence (rTPVang) expressed in percentage of movement duration were identified.

The whole-body movement (i.e., the body displacement and multi-joint coordination) was also analyzed. The body displacement (βbody) was computed as the angle of the whole body (ankle-head segment) relative to vertical (here, the direction normal to the cabin floor) at movement offset (Figure 3A). To identify multi-joint coordination, the coordination between ankle and hip joints was examined, using the Continuous Relative Phase analysis (CRP; Bardy et al. 1999; Hamill et al. 2012). For each trial, ankle and hip phase angles were expressed through a parametric phase plot where the normalized angular positions were plotted relative to the normalized angular velocity. Then, the calculated CRP corresponded to: $CRP(t) = \varphi_1(t) - \varphi_2(t)$ where $\varphi_1(t)$ and $\varphi_2(t)$ are the normalized phase angles for ankle and hip, respectively. Finally, the CRP was scaled from 0° to 180° where a CRP(t) < 90° indicates a preferential 'ankle strategy' (ankle and hip moving in-phase) while a CRP(t) > 90° indicates a 'hip strategy' (ankle and hip moving in anti-phase). Regarding the large variability whole-body organization between participants, we extracted a single variable by computing for each trial the relative time spent by participants using hip strategy (rTHS; expressed in percentage of total movement duration).

To identify the quantitative changes of EMG activity, an EMG root mean square (RMS) was computed on the four agonist muscles (TA, RA, DA, BB). First, raw EMG data were band-pass filtered with a Butterworth-type filter (cut-off frequency: 20-400 Hz; order: 4) centered around the mean and rectified. Then, a low-pass Butterworth filter (cut-off frequency: 3 Hz; order: 3) was applied twice (forward and backward to remove phase shift) to create an envelope

of the EMG signal (Hug 2011). The activity of each muscle was normalized and expressed as a percentage of their maximum activity observed during Tclose trials in normogravity (i.e., baseline condition without disturbance). The pre-activation time (before movement onset) of EMG activity was identified when EMG signal exceeded 10% of its peak in the trial. From this pre-activation time, the RMS was computed on a 200 ms window. Computing the RMS over this time window provided information regarding the changes in motor command before movement onset.

In addition, muscular synergies were analyzed, using a non-negative matrix factorization (NNMF). Raw EMG data were band-pass filtered with a Butterworth-type filter (cut-off frequency: 20-400 Hz; order: 4) centered around the mean and rectified. Then, a low-pass Butterworth filter (cut-off frequency: 10 Hz; order: 3; Hug 2011) was applied twice and the signal was normalized relative to the maximum value of each trial and time was normalized (2000 samples). NNMF was computed to identify muscle synergies from the eight muscles activity (See Tresch et al. 2006 for more details). Briefly, the EMGs were combined into an M × T matrix, where M represents the number of muscles (8 in this study) and T the number of EMG data points (2000) obtained in each trial. The NNMF decomposed the EMGs in a few synergies (< M). Each synergy can thus be described as a synergy vector W who represent the contribution level of each muscle (from 0 to 1) and a temporal activation pattern H of the synergy over the time (from 0 to 1). The difference between reconstructed and original EMGs was computed using the total variance (tVAF). The maximum iteration of NNMF algorithm was scaled at 1000 times for each number of synergies from 1 to 7 (number of muscles -1), until tVAF increase was < 0.05%. Finally, the number of synergies selected corresponded to a tVAF >90%.

Statistical analyses

To identify a potential effect of repeated exposure to gravitational changes across the successive parabolas, repeated-measure analyses of variance (ANOVAs) were used to compare the longitudinal endpoint error between each parabola (from 1 to 10) in the different environments (0g, 1.8g, 1g). Subsequently, repeated-measures ANOVAs including 3 environments (0g, 1.8g, 1g) x 2 targets (Tclose, Tfar) x 2 Perturbation conditions (Electro ON, Electro OFF) were performed on arm and whole-body kinematics and RMS EMG variables. Repeated-measure ANOVAs were performed using Statistica software (StatSoft, Inc.). The normal distribution of data for each variable was confirmed by Kolmogorov–Smirnov tests. Posthoc analyses were carried out using Newman–Keuls tests and significance threshold was set at $p < 0.05$.

To determine whether muscular synergies changed regarding the gravitational context, a statistical parametric mapping (SPM) was used. SPM analysis allowed a statistical comparison on the whole time-series of each synergy. Whitin-subject ANOVA was conducted on each synergy (1 to 3) for the 3 environments (0g, 1.8g, 1g). SPM analyses were computed in Matlab (MathWorks Inc., Natick, MA) using the open-source software package spm1D (version: M.0.4.7; www.spm1d.org). Significance threshold was set at $p < 0.05$. Posthoc analyses were performed using SPM paired t-test (0g vs. 1.8g, 0g vs. 1g, 1g vs. 1.8g). Bonferroni correction was used to reduce the statistical risk caused by the multiple tests across these three pairs.

RESULTS

Stability of reaching accuracy across parabolas

The longitudinal endpoint errors were first compared between each parabola (from 1 to 10) in the different environments (0g, 1.8g, 1g) to identify a potential effect of repeated exposure to gravitational changes across the successive parabolas. The ANOVA performed on

longitudinal endpoint error showed a significant main effect of Environment ($F_{(2, 16)} = 48.96$; $p < 0.001$) and a significant interaction between Environment x Parabola ($F_{(18, 144)} = 3.09$; $p < 0.001$). However, post-hoc analyses revealed that endpoint accuracy in 1.8g only differed in parabola 1 relative to the others ($p < 0.05$). but no difference was found between each other parabolas, whatever the environment. Specifically, while participants systematically undershot the targets in 1.8g compared to 0g and 1g, this undershot was significantly higher during the first parabola. To exclude this phenomenon presumably due to initial exposure from subsequent analyses and to focus the investigation on the motor adjustments regarding the gravitational level, data from the first parabola were removed and will be discussed elsewhere.

Endpoint accuracy and arm angular elevation

As also observed in 1g, participants reached accurately the target in 0g while they made more final errors in 1.8g. The ANOVA performed on longitudinal endpoint error showed a significant main effect of Environment ($F_{(2, 16)} = 49.77$; $p < 0.001$; Figure 2). Longitudinal endpoint error in 1.8g (-2.21 ± 1.17 cm) was greater than in 0g (0.14 cm ± 0.6; $p < 0.001$) and 1g (0.6 cm ± 0.97; $p < 0.001$). No other significant main effect or interaction was found with the other factors (Target: $p = 0.61$; Perturbation: $p = 0.23$; Environment × Target: $p = 0.1$; Environment x Perturbation: $p = 0.98$; Target x Perturbation: $p = 0.81$; Environment x Target x Perturbation: $p = 0.85$).

Participants modified the organization of arm elevation only in 0g with respect to 1g. The ANOVA performed on PVang showed a significant main effect of Environment ($F_{(2, 16)} = 30.61$; $p < 0.001$), Target ($F_{(1, 8)} = 81{,}2$; $p < 0.001$) and Perturbation ($F_{(1, 8)} = 8.3$; $p < 0.05$; Figure 3A). PVang was lower in 0g (369.04 $deg.s^{-1}$ ± 73.15) than 1g (423.53 $deg.s^{-1}$ ± 61.09; $p < 0.001$) and 1.8g (433.23 $deg.s^{-1}$ ± 62.5; $p < 0.001$). Moreover, PVang was higher towards Tclose (453.79 $deg.s^{-1}$ ± 47.95) than Tfar (363.4 $deg.s^{-1}$ ± 61.18; $p < 0.001$) and higher when the electromagnet was switched on (417.6 $deg.s^{-1}$ ± 71.04) than when it was switched off (399.61

deg.s^{-1} ± 70.67; $p < 0.05$). No significant interaction was found between these factors (Environment × Target: $p = 0.26$; Environment x Perturbation: $p = 0.21$; Target x Perturbation: $p = 0.61$; Environment x Target x Perturbation: $p = 0.66$). Comparable findings were found for the temporal organization of arm elevation. The ANOVA performed on rTPVang showed a significant main effect of Environment ($F_{(2, 16)} = 8.28$; $p < 0.01$), Target ($F_{(1, 8)} = 49.85$; $p < 0.001$) and Perturbation ($F_{(1, 8)} = 5.49$; $p < 0.05$; Figure 3B). rTPVang was lower in 0g (29.53 % ± 5.46) than 1g (32.93 % ± 4.94; $p < 0.001$) and 1.8g (32.03 % ± 4.87; $p < 0.001$). Moreover, rTPVang was lower towards Tfar (28.35 ± 4.34; $p < 0.001$) than Tclose (34.64 % ± 4.09) and lower when the electromagnet was switched on (31.04 % ± 5.45; $p < 0.05$) than when it was switched off (31.96 % ± 5.06). No significant interaction was found between these factors (Environment × Target: $p = 0.21$ Environment x Perturbation: $p = 0.79$; Target x Perturbation: $p = 0.95$; Environment x Target x Perturbation: $p = 0.79$).

The ANOVA performed on arm MD showed a significant main effect of Environment ($F_{(2, 16)} = 42.38$; $p < 0.001$), Target ($F_{(1, 8)} = 126.74$; $p < 0.001$) and a significant interaction between Environment x Target ($F_{(2, 16)} = 12.19$; $p < 0.001$). MD was higher in 0g (612.57 ms ± 105.07; $p < 0.001$) than 1g (524.30 ms ± 77.79; $p < 0.001$) and 1.8g (518.82 ms ± 79.38; $p < 0.001$). Obviously, MD was higher towards Tfar (613.06 ms ± 89.59; $p < 0.001$) than Tclose (490.73 ms ± 59.66; $p < 0.001$).

Whole-body kinematics

While Tclose trials were set to study arm kinematics only, Tfar trials were performed to study whole-body reaching (i.e., multi-joint organization). As for the kinematic changes reported for the arm movement, whole-body reorganizations were only present in 0g compared to 1g. The ANOVA performed on βbody showed a significant main effect of Environment ($F_{(2, 16)} = 27.77$; $p < 0.001$; Figure 4B). When participants reached towards Tfar, βbody was higher in 0g (12.98 deg ± 3.1) than 1g (9.14 deg ± 1.88; $p < 0.001$) and 1.8g (9.52 deg ± 2.36; $p <$

0.001). No other significant main effect or interaction was found with the other factors (Perturbation: $p = 0.31$; Environment x Perturbation: $p = 0.26$)

The ANOVA performed on the relative time spent by participants using a “hip strategy” (rTHS) showed a significant main effect of Environment ($F_{(2, 16)} = 8.61$; $p < 0.01$; Figure 4C). rTHS was lower in 0g (40.78 % ± 8.36) than 1g (48.8 % ± 10.47; $p < 0.01$) and 1.8g (51.21 % ± 8.76; $p < 0.01$). No other significant main effect or interaction was found with the other factors (Perturbation: $p = 0.47$; Environment x Perturbation: $p = 0.26$).

EMG analysis

While arm and whole-body reorganizations seemed to occur only in 0g compared to 1g, the analysis of muscular activity revealed deeper changes regarding the different gravitational constraints. The first part of EMG analysis focused on four muscles agonist muscles (TA, RA, DA, BB). The ANOVA performed on *tibialis anterior* (TA) RMS showed a significant main effect of Environment ($F_{(2, 16)} = 10.15$; $p < 0.01$) and Target ($F_{(1, 8)} = 29.98$; $p < 0.001$; Figure 5A). Muscular activity of TA was lower in 0g (280.05 a.u. ± 151.18) than 1g (422.38 a.u. ± 111.83; $p < 0.01$) and 1.8g (354.21 a.u. ± 124.97; $p < 0.05$) and lower in 1.8g than 1g ($p < 0.05$). Additionally, TA was less active when reaching towards Tclose (282.27 a.u. ± 97.04) than Tfar (422,15 a.u. ± 145.48; $p < 0.001$). No other significant main effect or interaction was found with the other factors (Perturbation: $p = 0.82$; Environment x Perturbation: $p = 0.64$; Target x Perturbation: $p = 0.70$; Environment x Target x Perturbation: $p = 0.75$). The ANOVA performed on *rectus abdominis* (RA) RMS showed a significant main effect of Target ($F_{(1, 8)} = 24.97$; $p < 0.01$; Figure 5B). The RA RMS was higher for Tfar (450.78 a.u. ± 207.12) than Tclose (343.03 a.u. ± 130.78; $p < 0.01$). No other significant main effect or interaction was found with the other factors (Environment: $p = 0.98$; Perturbation: $p = 0.21$; Environment x Target: $p = 0.25$; Environment x Perturbation: $p = 0.95$; Target x Perturbation: $p = 0.55$; Environment x Target x Perturbation: $p = 0.4$). The ANOVA performed on *biceps brachii* (BB) RMS showed a

significant main effect of Environment ($F_{(2, 16)} = 4.17$; $p < 0.05$), Target ($F_{(1, 8)} = 7.36$; $p < 0.05$) and Perturbation ($F_{(1, 8)} = 5.37$; $p < 0.05$; Figure 5C). BB RMS was lower in 0g (215.82 a.u. ± 83.27) than 1.8g (280.23 a.u. ± 122.76; $p < 0.05$) and close to significance with respect to 1g (264. 85 a.u. ± 77.29; $p = 0.051$). Moreover, BB RMS was lower when reaching towards Tfar (226.58 a.u. ± 83.58) than Tclose (280.69 a.u. ± 107.4; $p < 0.05$) and higher when the electromagnet was switched on (270.52 a.u. ± 109.18) than switched off (236.75 a.u. ± 86.66; $p < 0.05$). No interaction was found with the other factors (Environment x Target: $p = 0.89$; Environment x Perturbation: $p = 0.16$; Target x Perturbation: $p = 0.79$; Environment x Target x Perturbation: $p = 0.44$). Finally, the ANOVA performed on *deltoid anterior* (DA) RMS showed a significant main effect of Target ($F_{(1, 8)} = 5.95$ $p < 0.05$; Figure 5D). The RMS was higher for Tclose (285.74 a.u. ± 104.46) than Tfar (258.15 a.u. ± 87.93; $p < 0.05$). No other significant main effect or interaction was found with the other factors (Environment: $p = 0.06$; Perturbation: $p = 0.49$; Environment x Target: $p = 0.68$; Environment x Perturbation: $p = 0.3$; Target x Perturbation: $p = 0.08$; Environment x Target x Perturbation: $p = 0.98$).

Muscular synergies

The NNMF computed on the 8 muscles highlighted 3 main synergies reflecting the whole reaching movement (Figure 6C). Synergy 1 appeared before movement onset and mainly involved the TA and the RA (Figure 6A,6B). Synergy 2 was present around movement onset and close to movement offset and mainly involved the DA and the BB. Synergy 3 involved mainly the SL, the ES, the DP, and the TB around movement offset. The repeated measures ANOVA conducted with SPM analysis revealed a significant effect of Environment ($F_{(2, 16)} = 8.164$) only for the synergy 1. The significant threshold was reached three times: before movement onset ($p < 0.001$), straight after movement onset ($p < 0.001$) and close to movement offset ($p < 0.001$). However, post hoc analyses with Bonferroni correction showed no significant difference ($p > 0.02$).

DISCUSSION

The present study investigated how motor control of whole-body reaching is impacted by microgravity and hypergravity contexts generated by means of parabolic flights. By analyzing endpoint accuracy, our results showed that motor performance was maintained in 0g while systematic undershots were found in 1.8g. Arm and whole-body kinematics as well as EMG analyses revealed modifications of motor planning in 0g compared to 1g but little changes in 1.8g. This may suggest that hypergravity is a more challenging environment than microgravity. Also, applying a small mechanical perturbation at movement initiation did not overall impair reaching with respect to unperturbed trials in each environment, thus reflecting preserved motor flexibility.

Distinct adapted states in line with the environmental requirements.

The absence of gravity did not affect whole-body reaching performance in terms of final spatial accuracy, as previously reported (Macaluso et al. 2017). This is consistent with previous work (Bringoux et al. 2012; Crevecoeur et al. 2009b; Macaluso et al. 2017; Papaxanthis et al. 2005) suggesting that the optimal integration of novel body and arm dynamics prior to movement onset allowed the CNS to produce a motor command perfectly scaled to gravitational constraints. This adapted state had a direct influence on spatiotemporal organization of arm movement. In line with a previous study (Macaluso et al. 2017), participants exhibited an earlier relative time to peak velocity which corresponded to a larger deceleration part relative to movement duration. A longer deceleration phase may help better process sensory feedback to maintain endpoint accuracy (Sarlegna et al. 2003; Terrier et al. 2011). Macaluso et al. (2017) tested participants on the same task but only during microgravity episodes and without mechanical perturbations. They did not report any other modification of velocity parameters or movement duration while the present study revealed a lower peak velocity of angular arm elevation and a longer movement duration in microgravity. Some studies also reported a

reduction of movement speed in microgravity, which may reflect participants' strategy to favor accuracy over speed when facing new gravitational constraints (Crevecoeur et al. 2010; Mechtcheriakov et al. 2002). In our experiment, such a cautious strategy could be explained by the increased uncertainty caused by successive micro vs hypergravity episodes during which the task was performed, and the unexpected mechanical constraint which could be present or not at movement initiation.

The analysis of spatial accuracy in hypergravity revealed a systematic undershot compared to micro and normogravity. Some studies also reported undershots in hypergravity and suggested that, prior to movement onset, motor commands are still scaled to 1g and consequently, the force produced to reach the target is too weak in 1.8g (Cohen and Welch 1992; Ross 1991). However, we found muscular adjustments before movement onset, suggesting early changes according to the hypergravity context at the motor planning stage. Also interestingly, the mean of endpoint deviations appeared very close to the accuracy limits defined by the targets (i.e., dotted line; Figure 2). Therefore, cognitive factors could explain these observed undershots (Crevecoeur et al. 2009a), as participants might tend to minimize energy cost by staying at the limit of the goal task (i.e., "reach the target as fast and as accuracy as possible").

The optimal control theory (Todorov 2004; Todorov and Jordan 2002) could bring a good explanation of these different motor performance. Whatever the environment, optimality rules usually consist in minimizing energy costs (i.e., by the optimization of muscular activation) while maximizing the task success (i.e., by the reduction of endpoint error). Based on this compromise, different environments may lead to different motor performance. The absence of gravitational constraints implies a decrease of muscular activity that favors the minimization of energy costs, thus allowing the maximization of success task. Conversely in hypergravity, the higher gravitational constraint involves higher muscle activations. In this

context, minimizing energy costs involves a reevaluation of the task success. By pointing near the limits defined by the target, participants might have considered the task still successful and conversely avoided to increase energy costs to maintain the same level of accuracy.

Whole-body reorganization

As previously reported, we found that whole-body reaching movements in microgravity involved whole-body reorganization (i.e., higher body displacement; Casellato et al. 2012; Macaluso et al. 2017). Moreover, the analysis of hip and ankle joint coordination during movement execution revealed a simultaneous flexion which corresponds to a preference for "ankle strategy" (Horak and Nashner 1986) to regulate body bending. Because gravitational constraints acting upon the control of stance were absent, participants exceeded the physical limits of support surface and showed a larger forward body bending than in normogravity.

Contrasting with microgravity, maintaining balance in hypergravity involved a greater stiffness of leg joints (Ritzmann et al. 2015) which may lead to a reduced forward bending. In the present study, the whole-body organization observed in normogravity was maintained in hypergravity. Precisely, both forward trunk bending and hip and ankle joint coordination were comparable to that observed in normogravity. While this conservative behavior still allowed the participants to maintain balance, we hypothesize it made it difficult to produce an optimal reaching performance.

Changing gravitational contexts gives rise to functional muscular adjustments

The arm and whole-body kinematics adjustments appeared directly linked with context-specific muscular modifications. In microgravity, unloading reduces the necessity to produce a high torque at the elbow joint during whole-body reaching movements (Bringoux et al. 2020). Here, because forward body bending involves lower constraints at the ankle joint in microgravity, we observed the decrease of TA activation. The decrease of this muscle activity, specifically involved in body bending, could extend the previous finding at the ankle joint level.

On the other hand, only arm kinematics adjustments were found in hypergravity, as revealed by the increased BB activity before movement onset which allowed to counteract the greater gravitational acceleration. These findings also confirm that hypergravity constraints are integrated in a feedforward manner (Crevecoeur et al. 2009a), although insufficiently to perform as in normogravity baseline.

Moreover, a task specific adjustment was found and could also be distinguished by the muscles activation. The analysis of antagonist muscles activation showed an increase of arm muscle (BB and DA) when participants reached towards the close target while leg and trunk muscles (TA and RA) decreased toward the far target. These differences could be explained by the shorter movement time necessary to reach the close target. Then, arm muscles were more activated before movement onset leading to quickly move the arm toward the target. Conversely, toward the far target, leg and trunk muscles were more activated before movement onset to initiate the body bending while arm muscles were activated later, after movement onset.

Preserved muscular synergies across different gravitational contexts

We analyzed muscular synergies to investigate the possible dimensional reduction operated by the CNS to produce complex movements (d'Avella et al. 2006). Based on an analysis of the activations of eight muscles, three main synergies corresponded to the three main steps of the whole-body reaching movement. The first synergy (Synergy 1) involved an activation of TA and RA before movement onset. These leg and trunk muscles activation allowed to prepare the trunk bending necessary to reach the far target. The second synergy (Synergy 2) appeared at the movement onset and involved an activation of DA, RA and BB. These agonist muscles allowed to produce both the trunk bending and the arm elevation. The third synergy (Synergy 3) appeared at the end of movement and involved an activation of two groups of muscles. The TB and DP were antagonist to the reaching movement. There activations allowed to slow down the arm elevation at the approach of target. In parallel, the

activation of leg and trunk antagonist muscles (SOL, RA and ES) kept the final position while body was bended forward.

This qualitative analysis of muscular synergies gives a global description of temporal and spatial muscular activity. Interestingly, the number of synergies which best explained all muscular activations remained the same despite the great difference between each gravitational context. During an arm cycling task, Botzheim et al. (2021) studied the effects of gravity by comparing two cycling positions (i.e., sitting and supine position). They also found the same number of synergies between each position despite their considerable biomechanical differences. This conservative behavior despite the gravitational context could represent the key of motor performance. Rather than a specific muscular synergy for each constraint, the CNS would build a general scheme for movement coordination (Roh et al. 2012). Finally, by keeping the same synergies as observed in normogravity, the CNS could easily adjust the motor performance as, for instance, minimizing the energy cost induced by gravitational constraints.

Adapted states to gravity contexts led to perfectly scaled feedback responses.

Online motor corrections following an unexpected mechanical perturbation were still effective in 0g and 1.8g to maintain final reach accuracy with respect to movements achieved without perturbation. The perturbation produced on the wrist around movement onset was compensated by an increased BB activation, whatever the gravitational context. The main consequence of this perturbation was observed on kinematics where the angular velocity of arm elevation increased. In hypergravity, the increased of global stiffness (Ritzmann et al. 2015; not measured in this study) caused by the higher gravitational acceleration could favor the additional BB activation observed in perturbation condition. These observations are in line with the hypothesis that increasing the activity of arm muscles improves feedback gain and thereby the arm responses to sudden and unpredictable perturbations (Franklin et al. 2012). On the other hand, while microgravity required to deal with the absence of external forces, an additional

unexpected mechanical perturbation is not an obstacle to motor performance. On a similar task, Bringoux et al. (2020) reported a perfectly scaled feedback response when the target moved unexpectedly at movement onset. These findings also support those already observed with robotic devices (Cluff and Scott 2013; Crevecoeur and Scott 2013; Kimura and Gomi 2009) or modified gravitational forced fields (Bringoux et al. 2020; Chomienne et al. 2021) and confirm the strong link between feedforward and feedback control.

Conclusion

The present study provides new insights on motor performance of whole-body reaching movements in altered gravity. Based on different adapted states to gravitational contexts, the CNS would help maintain an optimal ratio between the minimization of energy cost and the maximization of endpoint accuracy. Despite distinct motor performance, an additional mechanical perturbation did not impair motor flexibility supporting a strong link between feedforward and feedback control. Yet, one might speculate that hypergravity represents a more challenging state that microgravity for human motor control.

References

d'Avella A, **Portone A**, **Fernandez L**, **Lacquaniti F**. Control of Fast-Reaching Movements by Muscle Synergy Combinations. *J Neurosci* 26: 7791–7810, 2006.

Bardy BG, **Marin L**, **Stoffregen TA**, **Bootsma RJ**. Postural coordination modes considered as emergent phenomena. *J Exp Psychol Hum Percept Perform* 25: 1284–1301, 1999.

Bock O, **Howard IP**, **Money KE**, **Arnold KE**. Accuracy of aimed arm movements in changed gravity. *Aviat Space Environ Med* 63: 994–998, 1992.

Botzheim L, **Laczko J**, **Torricelli D**, **Mravcsik M**, **Pons JL**, **Oliveira Barroso F**. Effects of gravity and kinematic constraints on muscle synergies in arm cycling. *J Neurophysiol* 125: 1367–1381, 2021.

Brindle TJ, **Nitz AJ**, **Uhl TL**, **Kifer E**, **Shapiro R**. Kinematic and EMG characteristics of simple shoulder movements with proprioception and visual feedback. *J Electromyogr Kinesiol* 16: 236–249, 2006.

Bringoux L, **Blouin J**, **Coyle T**, **Ruget H**, **Mouchnino L**. Effect of gravity-like torque on goal-directed arm movements in microgravity. *J Neurophysiol* 107: 2541–2548, 2012.

Bringoux L, **Macaluso T**, **Sainton P**, **Chomienne L**, **Buloup F**, **Mouchnino L**, **Simoneau M**, **Blouin J**. Double-Step Paradigm in Microgravity: Preservation of Sensorimotor Flexibility in Altered Gravitational Force Field. *Front Physiol* 11: 377, 2020.

Casellato C, **Tagliabue M**, **Pedrocchi A**, **Papaxanthis C**, **Ferrigno G**, **Pozzo T**. Reaching while standing in microgravity: a new postural solution to oversimplify movement control. *Exp Brain Res* 216: 203–215, 2012.

Chomienne L, **Blouin J**, **Bringoux L**. Online corrective responses following target jump in altered gravitoinertial force field point to nested feedforward and feedback control. *J Neurophysiol* 125: 154–165, 2021.

Cluff T, **Scott SH**. Rapid feedback responses correlate with reach adaptation and properties of novel upper limb loads. *J Neurosci* 33: 15903–15914, 2013.

Cohen MM, **Welch RB**. Chapter 7 Visual-Motor Control in Altered Gravity. In: *Advances in Psychology*. Elsevier, p. 153–175.

Crevecoeur F, **McIntyre J**, **Thonnard J-L**, **Lefèvre P**. Movement stability under uncertain internal models of dynamics. *J Neurophysiol* 104: 1301–1313, 2010.

Crevecoeur F, **McIntyre J**, **Thonnard J-L**, **Lefèvre P**. Gravity-dependent estimates of object mass underlie the generation of motor commands for horizontal limb movements. *J Neurophysiol* 112: 384–392, 2014.

Crevecoeur F, **Scott SH**. Priors engaged in long-latency responses to mechanical perturbations suggest a rapid update in state estimation. *PLoS Comput Biol* 9: e1003177, 2013.

Crevecoeur F, **Thonnard J-L**, **Lefèvre P**. Optimal Integration of Gravity in Trajectory Planning of Vertical Pointing Movements. *J Neurophysiol* 102: 11, 2009a.

Crevecoeur F, **Thonnard JL**, **Lefèvre P**. Forward models of inertial loads in weightlessness. *Neuroscience* 161: 589–598, 2009b.

Franklin S, **Wolpert DM**, **Franklin DW**. Visuomotor feedback gains upregulate during the learning of novel dynamics. *J Neurophysiol* 108: 467–478, 2012.

Gaveau J, **Berret B**, **Angelaki DE**, **Papaxanthis C**. Direction-dependent arm kinematics reveal optimal integration of gravity cues. *eLife* 5, 2016.

Gaveau J, **Grospretre S**, **Berret B**, **Angelaki DE**, **Papaxanthis C**. A cross-species neural integration of gravity for motor optimization. *Sci Adv* 7: eabf7800, 2021.

Gaveau J, **Paizis C**, **Berret B**, **Pozzo T**, **Papaxanthis C**. Sensorimotor adaptation of point-to-point arm movements after spaceflight: the role of internal representation of gravity force in trajectory planning. *J Neurophysiol* 106: 620–629, 2011.

Gomi H. Implicit online corrections of reaching movements. *Curr Opin Neurobiol* 18: 558–564, 2008.

Hamill J, **Palmer C**, **Van Emmerik REA**. Coordinative variability and overuse injury. *Sports Med Arthrosc Rehabil Ther Technol* 4: 45, 2012.

Hayashi T, **Yokoi A**, **Hirashima M**, **Nozaki D**. Visuomotor map determines how visually guided reaching movements are corrected within and across trials. *eNeuro* 3, 2016.

Horak FB, **Nashner LM**. Central programming of postural movements: adaptation to altered support-surface configurations. *J Neurophysiol* 55: 1369–1381, 1986.

Hug F. Can muscle coordination be precisely studied by surface electromyography? *J Electromyogr Kinesiol* 21: 1–12, 2011.

Kimura T, **Gomi H**. Temporal development of anticipatory reflex modulation to dynamical interactions during arm movement. *J Neurophysiol* 102: 2220–2231, 2009.

Macaluso T, **Bourdin C**, **Buloup F**, **Mille M-L**, **Sainton P**, **Sarlegna FR**, **Taillebot V**, **Vercher J-L**, **Weiss P**, **Bringoux L**. Kinematic features of whole-body reaching movements underwater: Neutral buoyancy effects. *Neuroscience* 327: 125–135, 2016.

Macaluso T, **Bourdin C**, **Buloup F**, **Mille M-L**, **Sainton P**, **Sarlegna FR**, **Vercher J-L**, **Bringoux L**. Sensorimotor reorganizations of arm kinematics and postural strategy for functional whole-body reaching movements in microgravity. *Front Physiol* 8: 821, 2017.

Mechtcheriakov S, **Berger M**, **Molokanova E**, **Holzmueller G**, **Wirtenberger W**, **Lechner-Steinleitner S**, **De Col C**, **Kozlovskaya I**, **Gerstenbrand F**. Slowing of human arm movements during weightlessness: the role of vision. *Eur J Appl Physiol* 87: 576–583, 2002.

Mierau A, **Girgenrath M**, **Bock O**. Isometric force production during changed-Gz episodes of parabolic flight. *Eur J Appl Physiol* 102: 313–318, 2007.

Mills KR. The basics of electromyography. *J Neurol Neurosurg Psychiatry* 76 Suppl 2: ii32-35, 2005.

Papaxanthis C, **Pozzo T**, **McIntyre J**. Kinematic and dynamic processes for the control of pointing movements in humans revealed by short-term exposure to microgravity. *Neuroscience* 135: 371–383, 2005.

Ritzmann R, **Freyler K**, **Krause A**, **Gollhofer A**. No Neuromuscular Side-Effects of Scopolamine in Sensorimotor Control and Force-Generating Capacity Among Parabolic Fliers. *Microgravity Sci Technol* 28: 477–490, 2016.

Ritzmann R, **Freyler K**, **Weltin E**, **Krause A**, **Gollhofer A**. Load Dependency of Postural Control - Kinematic and Neuromuscular Changes in Response to over and under Load Conditions. *PLOS ONE* 10: e0128400, 2015.

Roh J, **Rymer WZ**, **Beer RF**. Robustness of muscle synergies underlying three-dimensional force generation at the hand in healthy humans. *J Neurophysiol* 107: 2123–2142, 2012.

Ross HE. Motor skills under varied gravitoinertial force in parabolic flight. *Acta Astronaut* 23: 85–95, 1991.

Rousseau C, **Papaxanthis C**, **Gaveau J**, **Pozzo T**, **White O**. Initial information prior to movement onset influences kinematics of upward arm pointing movements. *J Neurophysiol* 116: 1673–1683, 2016.

Saijo N, **Gomi H**. Multiple motor learning strategies in visuomotor rotation. *PloS One* 5: e9399, 2010.

Sarlegna FR, **Blouin J**, **Bresciani J-P**, **Bourdin C**, **Vercher J-L**, **Gauthier GM**. Target and hand position information in the online control of goal-directed arm movements. *Exp Brain Res* 151: 524–535, 2003.

Sarlegna FR, **Mutha PK**. The influence of visual target information on the online control of movements. *Vision Res* 110: 144–154, 2015.

Telgen S, **Parvin D**, **Diedrichsen J**. Mirror reversal and visual rotation are learned and consolidated via separate mechanisms: recalibrating or learning de novo? *J Neurosci* 34: 13768–13779, 2014.

Terrier R, **Forestier N**, **Berrigan F**, **Germain-Robitaille M**, **Lavallière M**, **Teasdale N**. Effect of terminal accuracy requirements on temporal gaze-hand coordination during fast discrete and reciprocal pointings. *J Neuroengineering Rehabil* 8: 10, 2011.

Todorov E. Optimality principles in sensorimotor control. *Nat Neurosci* 7: 907–915, 2004.

Todorov E, **Jordan MI**. Optimal feedback control as a theory of motor coordination. *Nat Neurosci* 5: 1226, 2002.

Tresch MC, **Cheung VCK**, **d'Avella A**. Matrix Factorization Algorithms for the Identification of Muscle Synergies: Evaluation on Simulated and Experimental Data Sets. *J Neurophysiol* 95: 2199–2212, 2006.

White O, **Gaveau J**, **Bringoux L**, **Crevecoeur F**. The gravitational imprint on sensorimotor planning and control. *J Neurophysiol* 124: 4–19, 2020.

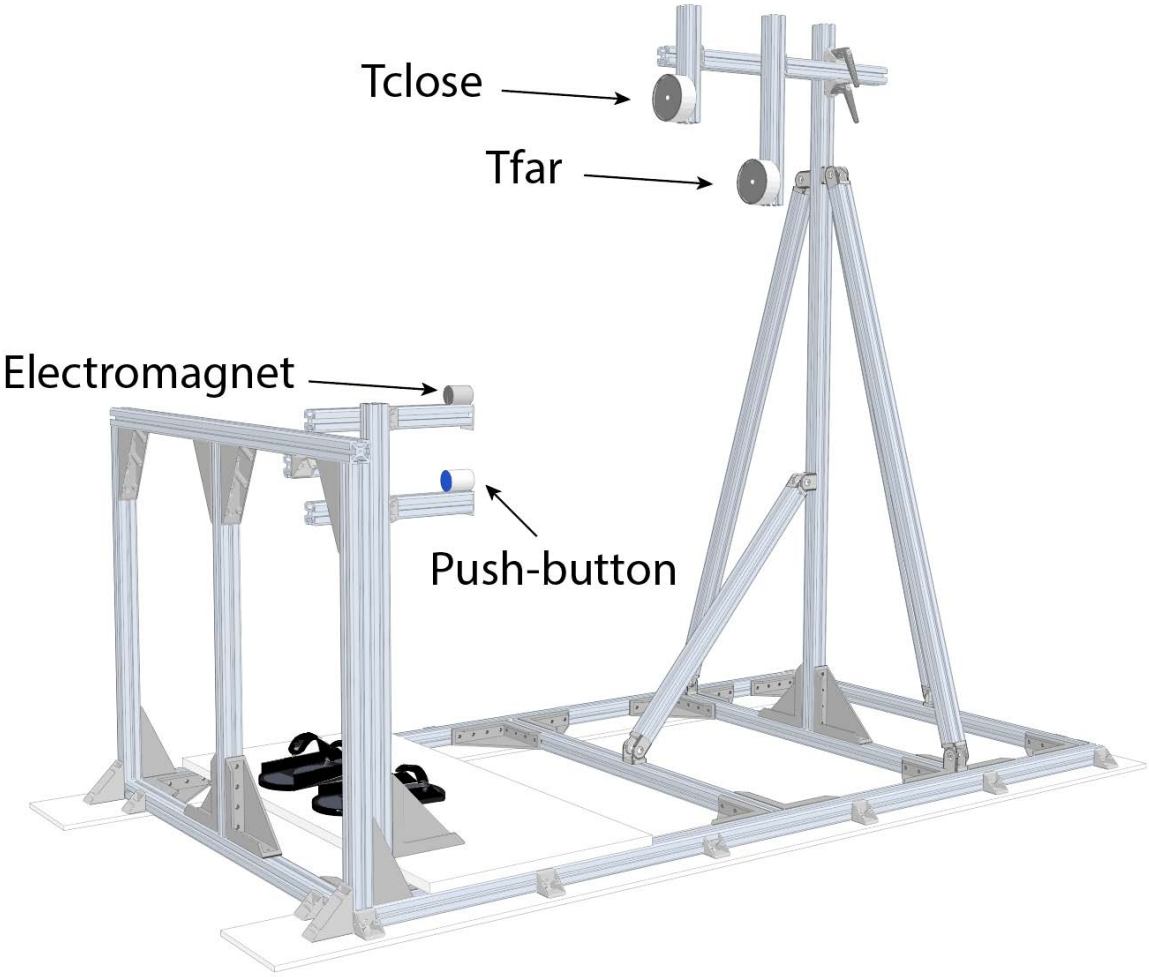

Figure 1: Global view of the pointing structure including the visual targets (Tclose and Tfar), the push-button to standardize the fingertip start position and the electromagnet to unexpectedly perturb reach movement initiation.

582

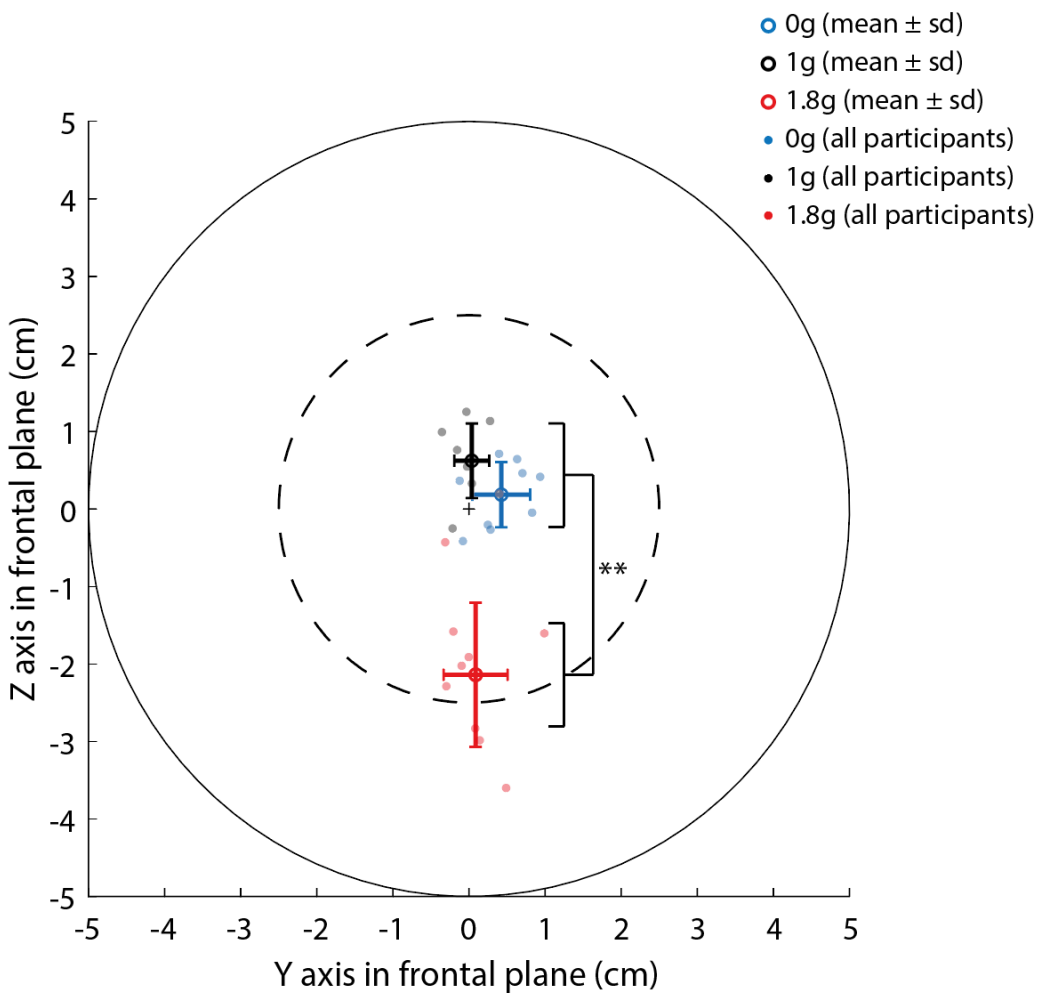

*Figure 2: Endpoint errors as a function of Environment. Reaching accuracy was impaired in 1.8g, leading to obvious undershots relative to the target center while no significant difference was found between 0g and 1g. **P<0.01.*

583

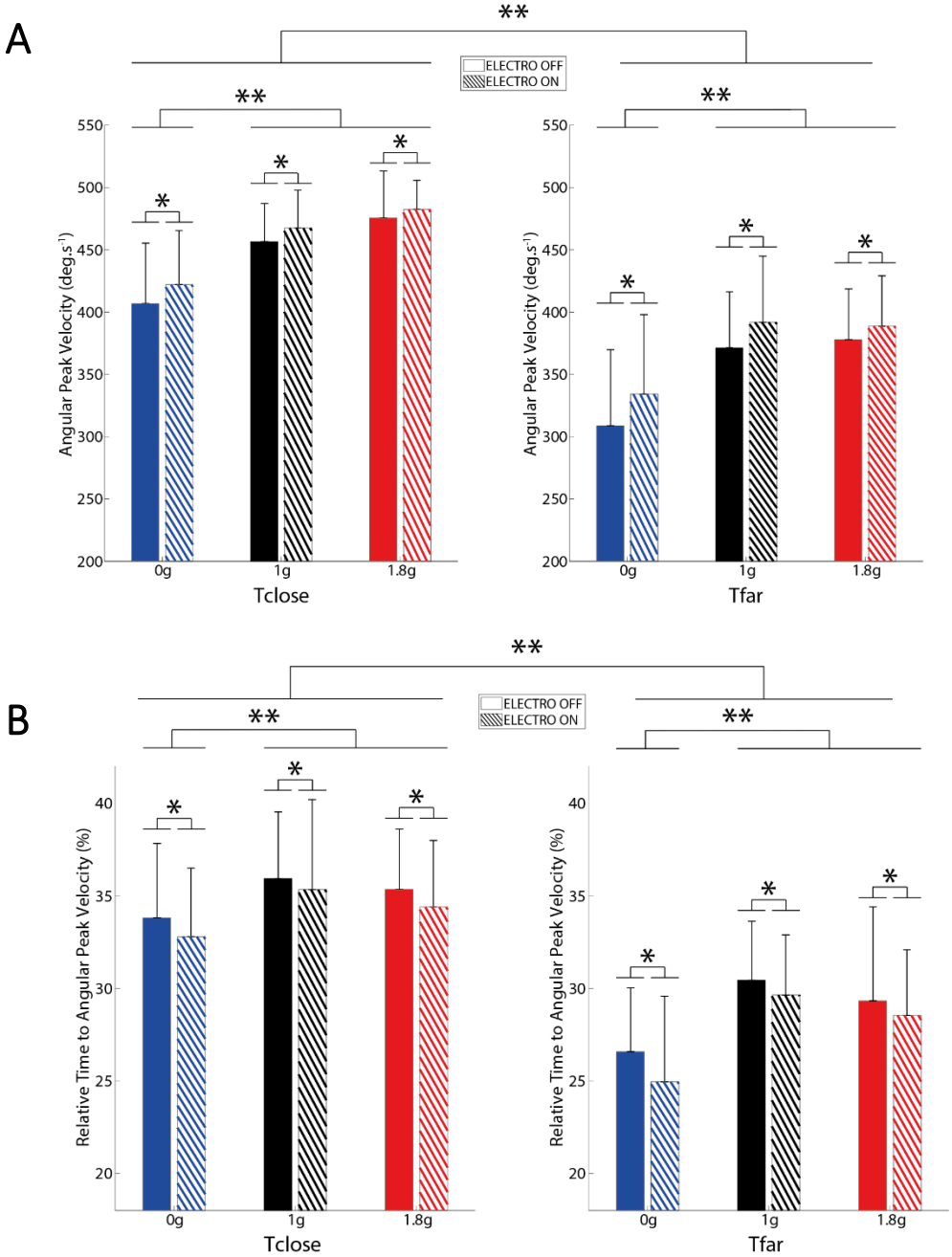

*Figure 3: Mean angular Peak Velocity (PVang - A) and rTPVang (B) relative to Environment, Target, and Perturbation The lower rTPVang observed in 0g corresponded to a higher relative deceleration time. *P<0.05, **P<0.01.*

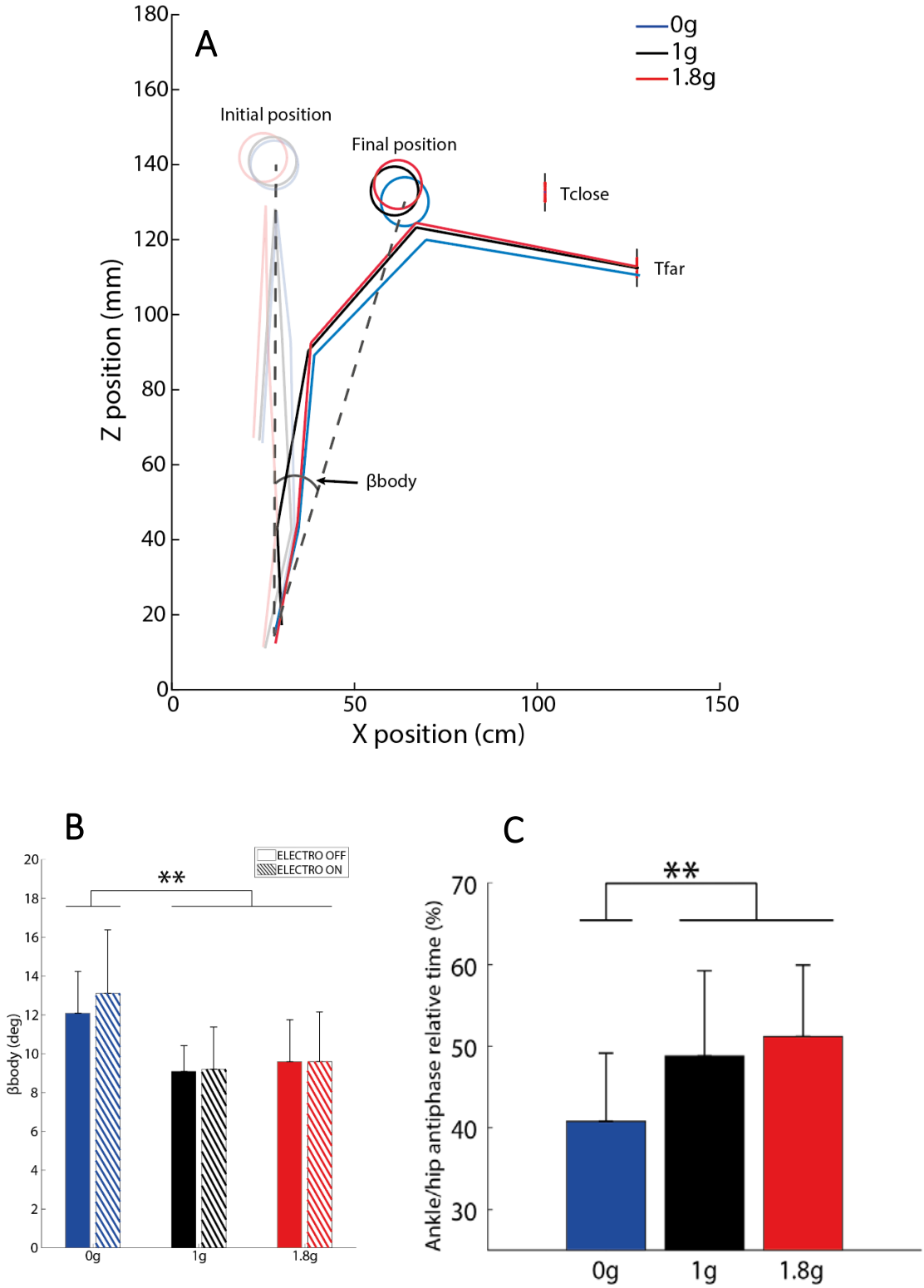

*Figure 4: Representative whole-body kinematics for a typical subject in micro-, hyper- and normogravity (A). Mean angular position of the ankle-head segment relative to vertical (βbody) as a function of the Environment, Target, and Perturbation (B). Mean relative time with hip strategy (rTHS) relative to Environment (C). Whole-body reorganizations were observed only in 0g where participants highlighted a larger forward body tilt relative to the vertical. Moreover, the lower ankle/hip antiphase relative time observed in 0g suggests that participants preferentially used an ankle strategy in absence of gravitational constraints. **P<0.01*

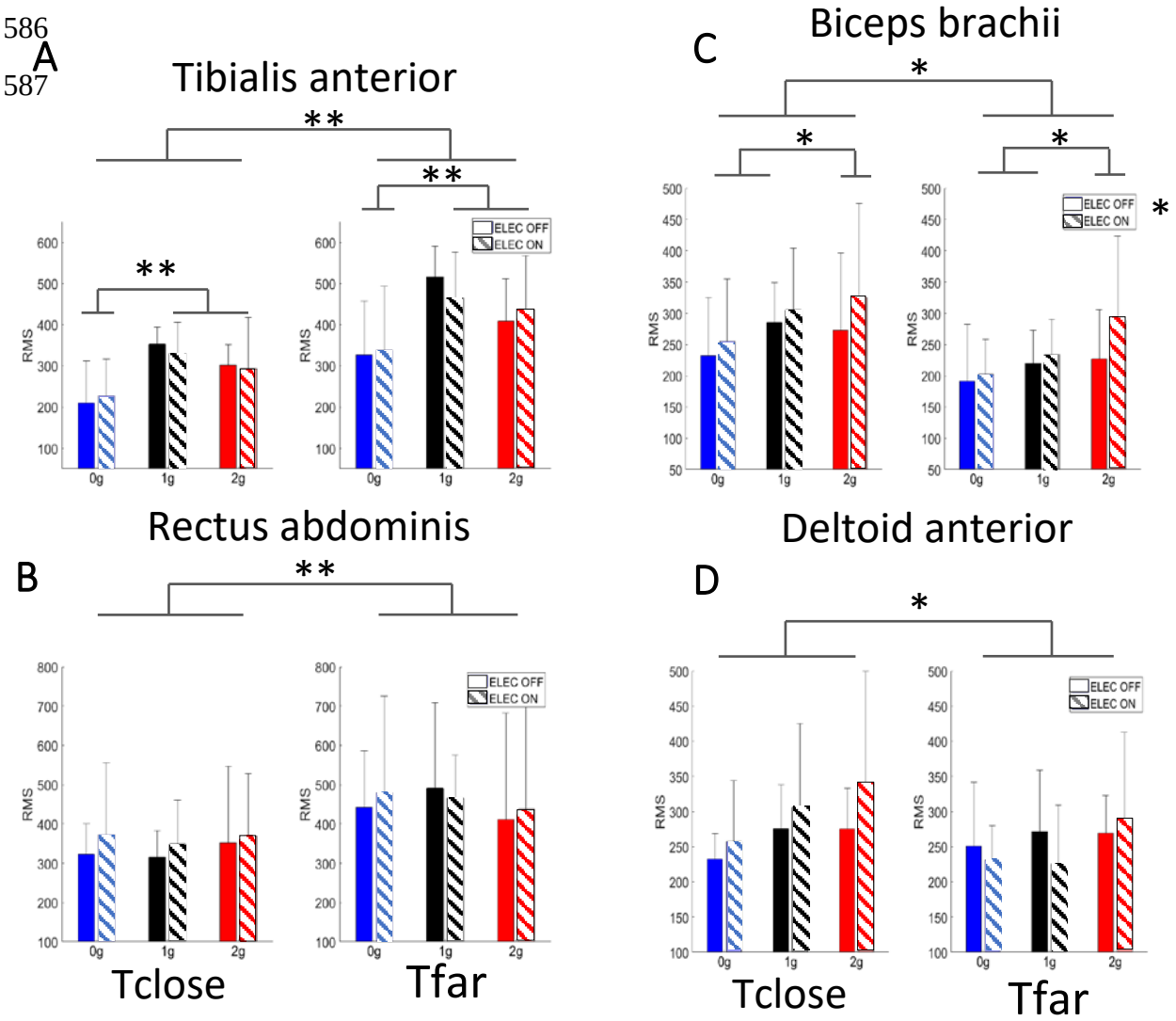

*Figure 5: Mean EMG root mean squares (RMS) of the 4 agonist muscles relative to Environment, Target, and Perturbation. All four muscles presented a significant difference between targets. While activity of leg muscles (TA and RA) was lower when reaching Tclose, reaching movements toward Tfar presented a higher activation of arm muscles (BB and DA). In addition, activity of TA and BB was lower in 0g than in the 1g and 1.8g. Finally, only BB had a higher activation when the electromagnet was switched on. *P<0.05; **P<0.01.*

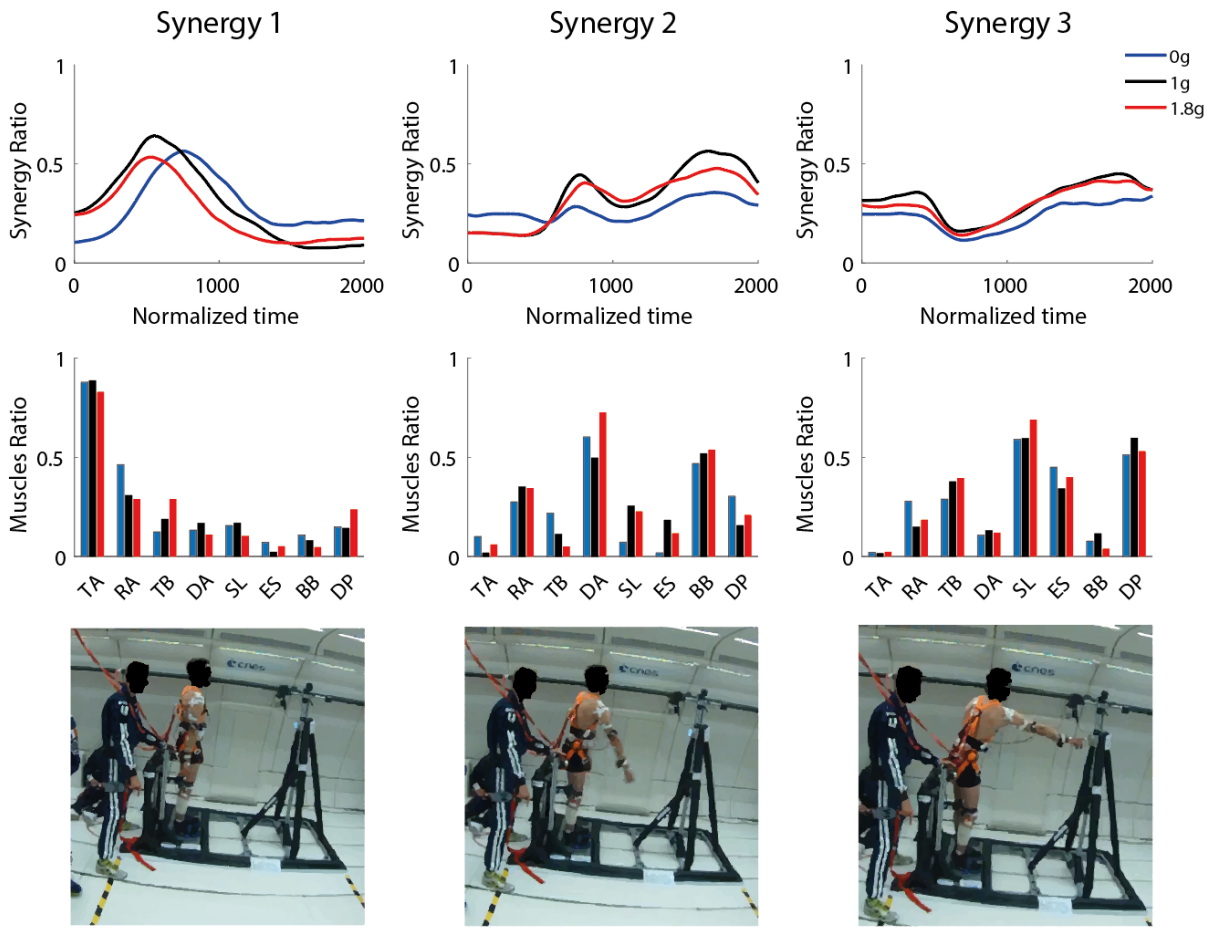

Figure 6: Mean muscular synergies for each environment (A). Mean muscle ratio for each environment (B). Illustration of the three steps of movement corresponding to the three muscular synergies (C). Synergy 1 corresponded to the preparation of movement with an activation of TA and RA before movement onset. Synergy 2 appeared at movement onset and mainly involved agonist muscles involved in reaching movement (DA, RA, BB) which allowed forward body tilt and arm elevation. Synergy 3 was mainly present at the end of movement where participants slowed down arm elevation by activating antagonist arm muscles (TB and DP) and kept the final position by activating leg and trunk muscles (SOL, RA and ES).